



PRESSURE DEPENDENT YIELD CRITERIA APPLIED FOR IMPROVING DESIGN PRACTICES AND INTEGRITY ASSESSMENTS AGAINST YIELDING OF ENGINEERING POLYMERS¹

Gustavo Henrique Bolognesi Donato²
Marcos Bianchi³

Abstract

Conventional yield criteria for ductile materials, such as Tresca and von Mises, predict that yielding is independent on the hydrostatic stress state (pressure), which means that tensile and compressive stress-strain behaviors are considered equal and are equally treated. This approach is reasonable for ductile metallic materials but sometimes inaccurate for polymers, which commonly present larger compressive yield strength, therefore being characterized as uneven. As a step in the direction of improving design practices taking advantage of unevenness, this work presents two key-activities: i) four selected polymers were tested under tension and compression to identify unevenness and assess its levels; ii) in the sequence, results were incorporated in adapted design practices using modified yield criteria. Results show that mass reductions up to 40% could be reached even with simple geometric changes, while keeping original safety and stiffness levels.

Key-words: Uneven polymers; Pressure dependent yield criteria; Experimental testing; Structural improvement.

CRITÉRIOS DE ESCOAMENTO DEPENDENTES DA TENSÃO HIDROSTÁTICA APLICADOS AO APRIMORAMENTO DO PROJETO E AVALIAÇÃO DE INTEGRIDADE AO ESCOAMENTO DE POLÍMEROS DE ENGENHARIA

Resumo

Critérios convencionais como de Tresca e von Mises admitem que o escoamento é independente do nível de tensão hidrostática e, portanto, idealizam os materiais como balanceados (mesmas propriedades em tração e compressão). Embora razoável para metais dúcteis, esta hipótese pode ser imprecisa para polímeros, os quais comumente apresentam maior resistência mecânica em compressão. A fim de aprimorar atividades de projeto tirando proveito do desbalanceamento, este trabalho apresenta duas atividades-chave: i) quatro polímeros selecionados foram ensaiados em tração e compressão para identificar a ocorrência e os níveis de desbalanceamento; ii) na sequência, os resultados foram incorporados em práticas adaptadas de projeto utilizando critérios de escoamento modificados. Os resultados apontam potencial de redução de massa de até 40% mesmo com alterações geométricas simples, mantidos os níveis de segurança e rigidez originais.

Palavras-chave: Polímeros desbalanceados; Critérios de escoamento dependentes da tensão hidrostática; Ensaios experimentais; Aprimoramento estrutural.

¹ Technical contribution to 66th ABM Annual Congress, July, 18th to 22th, 2011, São Paulo, SP, Brazil.

² Professor do Depto. de Engenharia Mecânica do Centro Universitário da FEI, gdonato@fei.edu.br

³ Mestre em Engenharia Mecânica pelo Centro Universitário da FEI, bianchimarcos@yahoo.com.br

1 INTRODUCTION

Classical plasticity theories and yield criteria for ductile materials, such as Tresca and von Mises original formulations,⁽¹⁾ include several assumptions, such as: i) the material is isotropic and homogeneous; ii) deformation proceeds under constant volume; iii) tensile and compressive yield strengths are equal; iii) yielding phenomenon is uninfluenced by the hydrostatic component of the stress state (pressure).⁽²⁾ Looking for the interest of this work, the last two assumptions mean that tensile and compressive stress-strain behaviors are identically treated in terms of structural integrity. This approach is reasonable for ductile metallic materials, but most times inaccurate for polymers, ceramics and even brittle metals. Engineering ductile thermoplastic polymers, which are focused here, usually present larger compressive yield strength if compared to conventional tensile yield strength, therefore being characterized as uneven polymers.^(2,3) This is a direct result of chains arrangement and deformation micromechanism, which are dependent on the hydrostatic stress level^(2,3) and will be briefly addressed later. The unevenness level in terms of yield strength is usually denoted “*m*” and is defined here as

$$m = \frac{\sigma_{ys-c}}{\sigma_{ys-t}}, \quad (1)$$

where σ_{ys-t} and σ_{ys-c} represents the yield strength under tension and compression.

In spite of being very scarce until the present days, some experimental results available in the literature including tensile and compressive stress-strain data reveal that unevenness for polymers usually presents levels between 20 % and 30 %.⁽⁴⁻⁷⁾ Additional results published by Jerabek, Steinberger e Major⁽⁸⁾ revealed, for polypropylene (PP), 50% larger yield strength under compression. An additional investigation conducted by the authors using the materials database of CES EDUPACK 2008 software⁽⁸⁾ revealed that, for the available 198 unfilled thermoplastic polymers, the unevenness ranges from $m \approx 0.60$ to $m \approx 7.00$ as shown by Figure 1(a). However, in most cases $1.00 \leq m \leq 2.00$ as can be realized in the same figure. Figure 1(b), in its turn, presents only some selected thermoplastic polymers of interest as a reference to the present work. In this evaluation, PA-66 presents approximately $0.90 \leq m \leq 1.60$, PA-6 presents $1.10 \leq m \leq 1.40$, PP presents $1.10 \leq m \leq 1.45$ and HDPE presents $0.95 \leq m \leq 1.50$.

Unfortunately, these uneven mechanical properties are in general not considered by current design and integrity assessment practices, conducting in most situations to excessively conservative structural solutions (and in some cases, nonconservative ones, as will be addressed later). This situation occurs because most of engineering teams are based on protocols developed during several decades for metallic materials, and which have been used with great success until nowadays. In the case of using new designs or new materials (such as polymers), existing uncertainties in the analytical models were usually overcome using larger safety factors. However, current market competitive context demands cost, lead times and mass reduction with, at the same time, quality and performance improvement (or, at least, maintenance). In the last fifteen to twenty years, the simple substitution of metallic components for polymeric ones, and the introduction of powerful finite element softwares provided huge amounts of gains in terms of new geometries and

mass reduction. In the present days, on the other hand, the benefits acquired are becoming saturated and day by day less representative and more laborious.

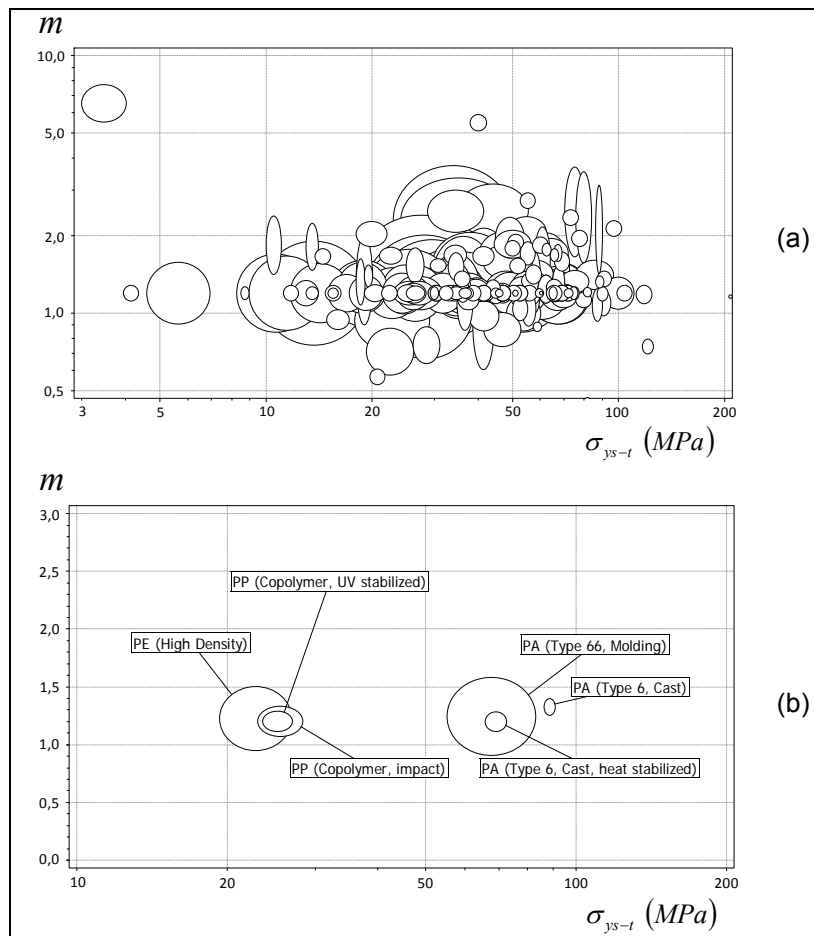


Figure 1. Yield strength unevenness under tensile and compressive loading for (a) 198 thermoplastic polymers available in CES EDUPACK 2008 software and (b) the same plot filtered for some polymers of interest for the present work. The bubbles represent results ranges available in the database.⁽⁹⁾

In this context, a reflection about the applicability and precision of classical yield criteria is mandatory in order to achieve additional gains with new materials. For uneven polymers, some pressure dependent yield criteria are available in the literature and consider the hydrostatic stress state and its effects on materials response in terms of yielding. The most popular criteria are the conically and parabolically modified von Mises theories,^(2,7) which will be presented in details and applied in the present work. From a design viewpoint, the application of these criteria in engineering activities can provide structural improvement by taking advantage of the larger compressive yield strength of polymers if used with numerical calculation techniques.

As a step in this direction, this work evaluates the effects of implementing pressure dependent yield criteria on design practices for components with regions working under compression. First, several polymers were uniaxially tested under tension/compression to obtain real stress-strain curves and unevenness levels. In the sequence, analytical and numerical calculations including optimization procedures were developed to incorporate the different criteria in the design process and assess stiffness, weight, stresses and safety factors of an example real component. The preliminary exploratory results show that the use of pressure dependent criteria in

design with the obtained data can reduce weight up to ~ 40 % keeping original stiffness and safety factors against yielding.

2 PRESSURE DEPENDENT YIELD CRITERIA

Several different pressure dependent yield criteria have been proposed, but most of them are based on the classic criterion proposed by Huber,⁽¹⁰⁾ Hencky⁽¹¹⁾ and Von Mises,⁽¹¹⁾ nowadays known as Von Mises, maximum octahedral shear stress or maximum strain energy criterion. It proposes that yielding occurs when the second invariant of the deviatoric stress tensor (J_2) reaches a critical value (k^2),⁽¹³⁾ in the form

$$J_2 = k^2 \quad , \quad (2)$$

where

$$J_2 = \frac{1}{6} [(\sigma_1 - \sigma_2)^2 + (\sigma_2 - \sigma_3)^2 + (\sigma_3 - \sigma_1)^2] \quad ; \quad k = \frac{1}{\sqrt{3}} \sigma_{ys-t} = 0,577 \cdot \sigma_{ys-t} \quad . \quad (3)$$

The classical Mises yield criterion is then presented by Eq. (4). Yielding occurs if Mises equivalent stress (σ_{vM}) is greater than tensile yield strength (σ_{ys-t}). The resulting yield locus for this criterion is presented by Figure 2(a), being σ_1 , σ_2 and σ_3 the three principal stresses. Since the hydrostatic stress (σ_h) can be written in terms of the first stress invariant (I_1) as presented by Eq. 5, it can be realized that there is no effect of σ_h on this failure prediction (the locus is characterized by a cylindrical tube aligned with the axis).

$$\sigma_{vM} = \frac{1}{\sqrt{2}} \sqrt{(\sigma_1 - \sigma_2)^2 + (\sigma_2 - \sigma_3)^2 + (\sigma_3 - \sigma_1)^2} \quad (4)$$

$$\sigma_h = \frac{I_1}{3} = \frac{\sigma_1 + \sigma_2 + \sigma_3}{3} \quad (5)$$

To include the pressure dependency on Mises original yield criterion, Hu and Pae⁽¹⁴⁾ proposed a methodology to include in Eq. (1) a second term depending on I_1 according to Eq. (6), which has proven to be a consistent approach.⁽¹³⁾ Expanding this formulation as a polynomial in I_1 and following the procedures presented by Ehrenstein and Erhard⁽¹⁵⁾ and Miller,⁽¹⁶⁾ Eqs. (7,8) can be found for $N = 1$ and $N = 2$ respectively. Equation (7) represents the conically modified von Mises (or Drucker-Prager) criterion, while Eq. (8) represents the parabolically modified von Mises criterion. In the conical model, Eq. (7) reveals that the effect of I_1 is linear, providing the yield surface shown by Figure 2(b). In the parabolic model, in its turn, Eq. (8) reveals that the effect of I_1 is quadratic, providing the yield surface shown by Figure 2(c). In both cases, the higher the compressive hydrostatic stress, the higher is the predicted yield strength, and yielding occurs when the modified equivalent stress is greater than the tensile yield strength, as stated by Eq. (9). Figure 3(a) presents a comparison between the original and the two modified yield criteria for plane stress conditions and two levels of unevenness (m). It can be realized that the conical model is more sensitive to high m values, which is expected due to the linear dependence on σ_h . However, the parabolic model is considered by some researchers as more realistic when compared to experimental results,⁽⁴⁻⁶⁾ which can be exemplified by Figure 3(b).

$$J_2 = k^2 + \sum_{i=0}^N \alpha_i \cdot I_1^i \tag{6}$$

$$\sigma_{vM-C} = \frac{1}{2m} \cdot \left[(m-1) \cdot (I_1) + (m+1) \sqrt{\frac{1}{2} [(\sigma_1 - \sigma_2)^2 + (\sigma_2 - \sigma_3)^2 + (\sigma_3 - \sigma_1)^2]} \right] \tag{7}$$

$$\sigma_{vM-P} = \frac{m-1}{2m} \cdot (I_1) + \sqrt{\left[\frac{m-1}{2m} \cdot (I_1) \right]^2 + \frac{1}{2m} [(\sigma_1 - \sigma_2)^2 + (\sigma_2 - \sigma_3)^2 + (\sigma_3 - \sigma_1)^2]} \tag{8}$$

$$\sigma_{vM-C} \leq \sigma_{LE-T} \quad ; \quad \sigma_{vM-P} \leq \sigma_{LE-T} \tag{9}$$

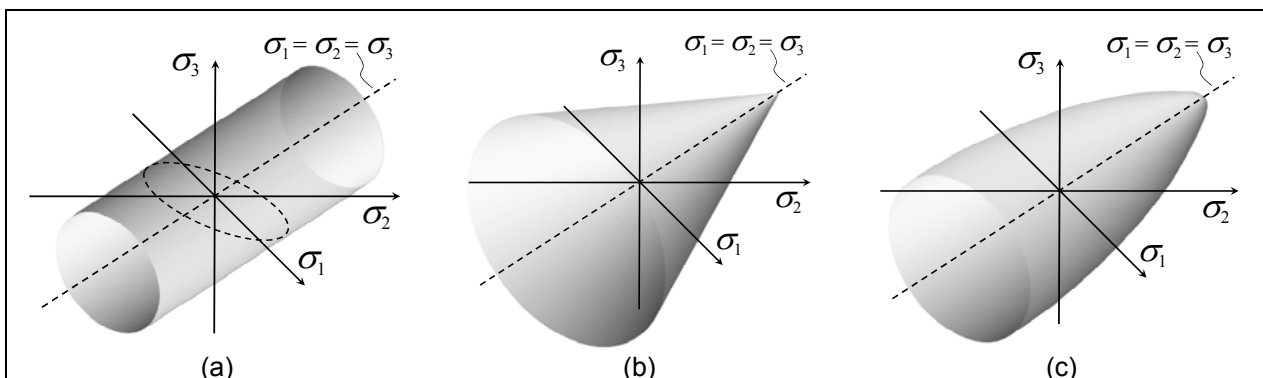


Figure 2. Illustrative yield surfaces plotted relative to the three principal axes considering (a) classical von Mises, (b) conically modified and (c) parabolically modified von Mises criterion.⁽²⁾

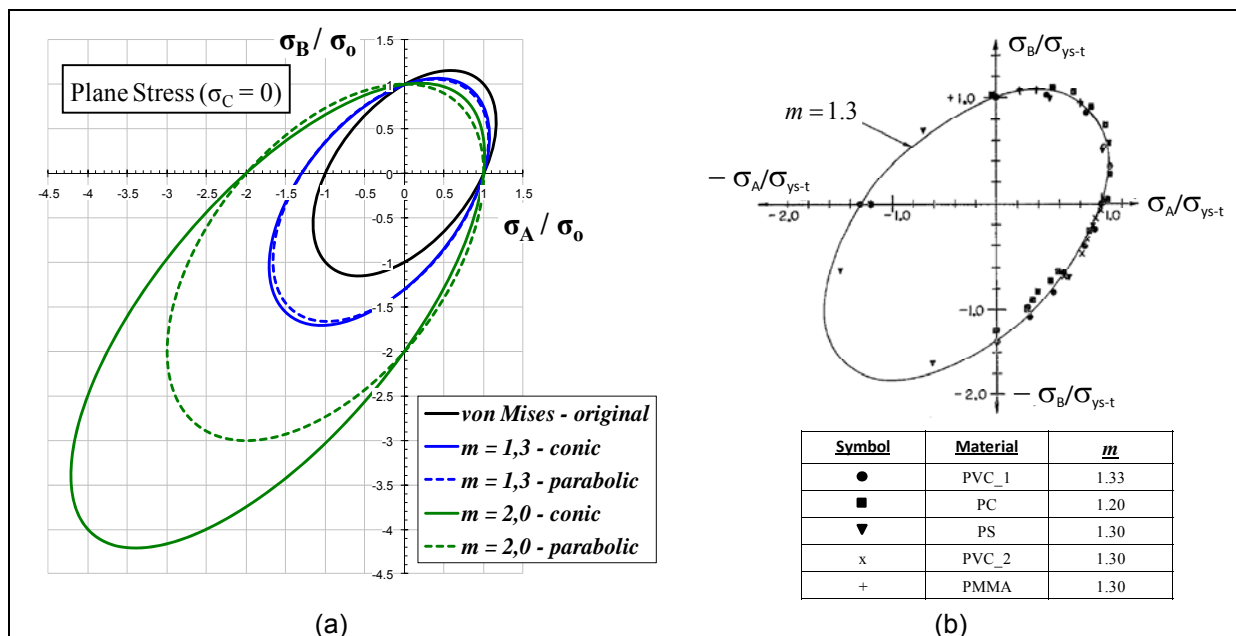


Figure 3. (a) yield loci for original von Mises criterion compared to conically and parabolically modified models for $m = 1,3$ and $m = 2,0$. (b) Experimental results compared to parabolic model prediction.⁽⁵⁾

3 TESTED MATERIALS AND EXPERIMENTAL PROCEDURES

Four thermoplastic polymers were tested under tension and compression, including PA-66, PA-6, PP and HDPE. All materials were purchased from polymers

distributors and came as round 3 meter long bars with 25.4 mm (1 inch) diameter. All specimens needed for each material were obtained from the same bar in order to avoid any shuffle or different batches. Figure 4 presents the dimensions and real examples of the tested specimens. All of them were machined parallel and with its centers aligned to the longitudinal axis of the bars, in order to sample the same material characteristics. Machining was conducted in CNC machines with small passes to avoid residual stresses or any damage to the raw material.

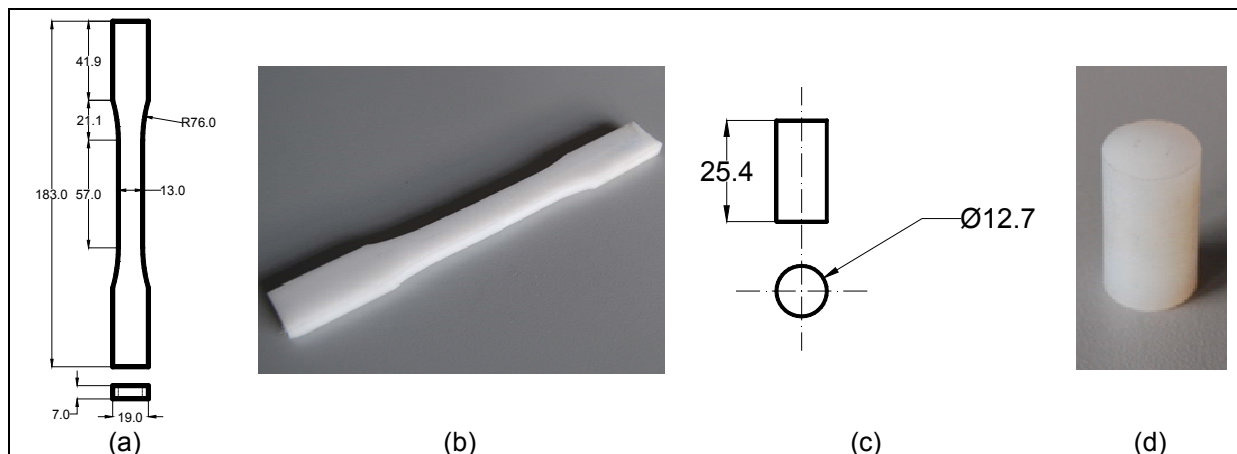


Figure 4. Dimensions and real example of tested specimens for (a,b) tension and (c,d) compression.

The specimens were kept and tested at 21 °C and 60 % relative humidity, using the same strain rate for tensile and compressive testing as recommended by ASTM D638⁽¹⁷⁾ for tension and ASTM D695⁽¹⁸⁾ for compression. Ten valid specimens were tested for each material (being 5 tensile and 5 compressive), and Table 1 presents specimens original dimensions, speeds of testing and corresponding strain rates. Tensile tests were conducted using a 30 kN electromechanical INSTRON testing machine (model 5567) and compressive tests using a 250 kN servohydraulic MTS testing machine (model 810). All results were acquired as ASCII files and post-processed using MS EXCEL and MATLAB platforms. Were determined for all specimens: i) elastic modulus (E); ii) offset yield strength ($\sigma_{ys-offset}$) considering 0.2, 0.5, 1.0 and 2.0 % plastic strain offsets ($\sigma_{ys-0.2}$, $\sigma_{ys-0.5}$, $\sigma_{ys-1.0}$ e $\sigma_{ys-2.0}$); iii) maximum yield strength ($\sigma_{ys-m\acute{a}x}$) based on the first point where $d\sigma/d\varepsilon = 0$; iv) tensile strength (σ_{uts}) as the overall maximum stress.

4 EXPERIMENTAL RESULTS AND DISCUSSION

Figure 5 presents stress-strain curves for all tested specimens considering engineering stress (σ) and strain (ε) data respectively under tension and compression. It can be realized that in most cases very good agreement was achieved between all five tested specimens for each material. Figure 6, in its turn, presents all tested specimens after final deformation or failure. Comparing representative tensile and compressive specimens, Figure 7 shows that yield strength unevenness clearly exists for PA-6, PP and HDPE, as will be detailed/quantified next.

Table 1: Initial valid dimensions, speeds of testing and strain rates for tensile and compression tests as recommended respectively by ASTM D638 (2008)⁽¹⁷⁾ and ASTM D695 (2008)⁽¹⁸⁾

Test	Initial valid length (mm)	Speed of testing (mm/min)	Initial strain rate (mm/mm/min)
Tension	50.0	2.55	0.051
Compression	25.4	1.30	0.051

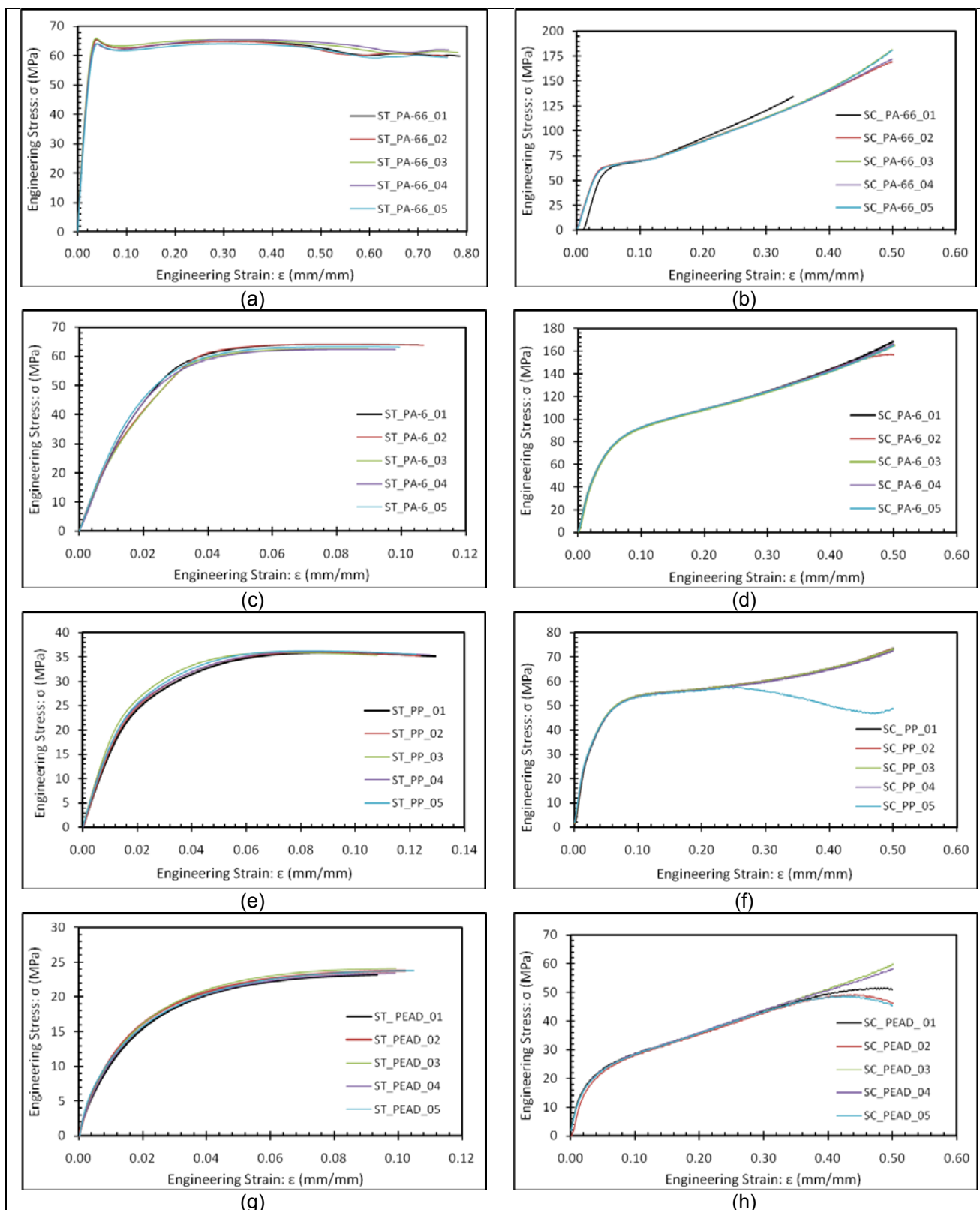

Figure 5. Stress-strain results under tension and compression respectively for (a,b) PA-66, (c,d) PA-6, (e,f) PP and (g,h) HDPE. It can be realized the general good agreement between multiple specimens.

Table 2 presents all post-treated results for elastic modulus, yield strength for different definitions and ultimate tensile strength. Unevenness levels were then calculated for both engineering (m_e) and true stress-strain (m_t) data.^(3,17,18) Considering the standard deviation, PA-66 can be considered even, while all other materials present relevant yield strength unevenness. Figure 8 presents the average values of (m_e) and (m_t) considering all the definitions of σ_{ys} . In spite of not being a physical measurement, these average values represent the unevenness behavior through elastic loading until plastic instability and are considered representative of the material (distinct) behavior under tension and compression. It can be realized that there exist a relevant difference between using engineering and true stress-strain data. Results based on true data reveals less unevenness and are considered here as more realistic due to the large strain response of polymers even for low stress levels.

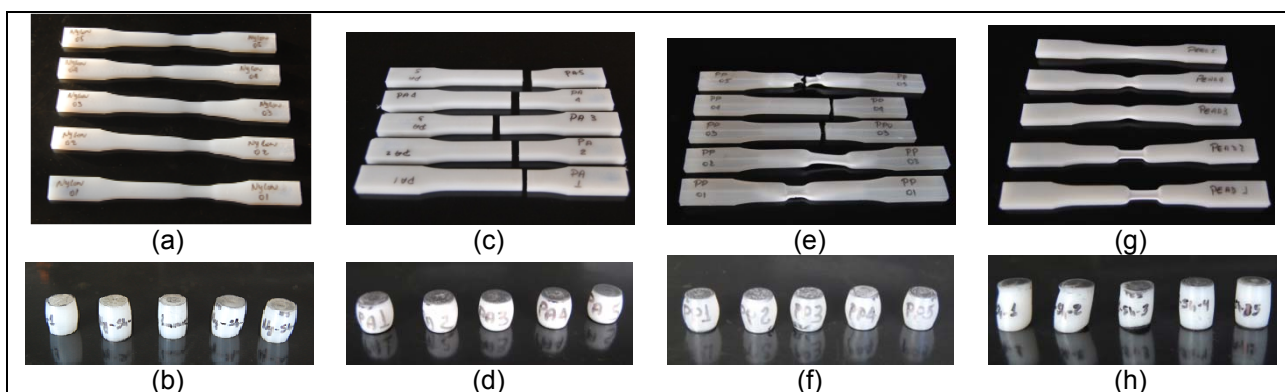


Figure 6. Tensile and compressive specimens after testing for (a,b) PA-66, (c,d) PA-6, (e,f) PP and (g,h) HDPE. The grey color at the top of compression specimens is due to lubrication residues.

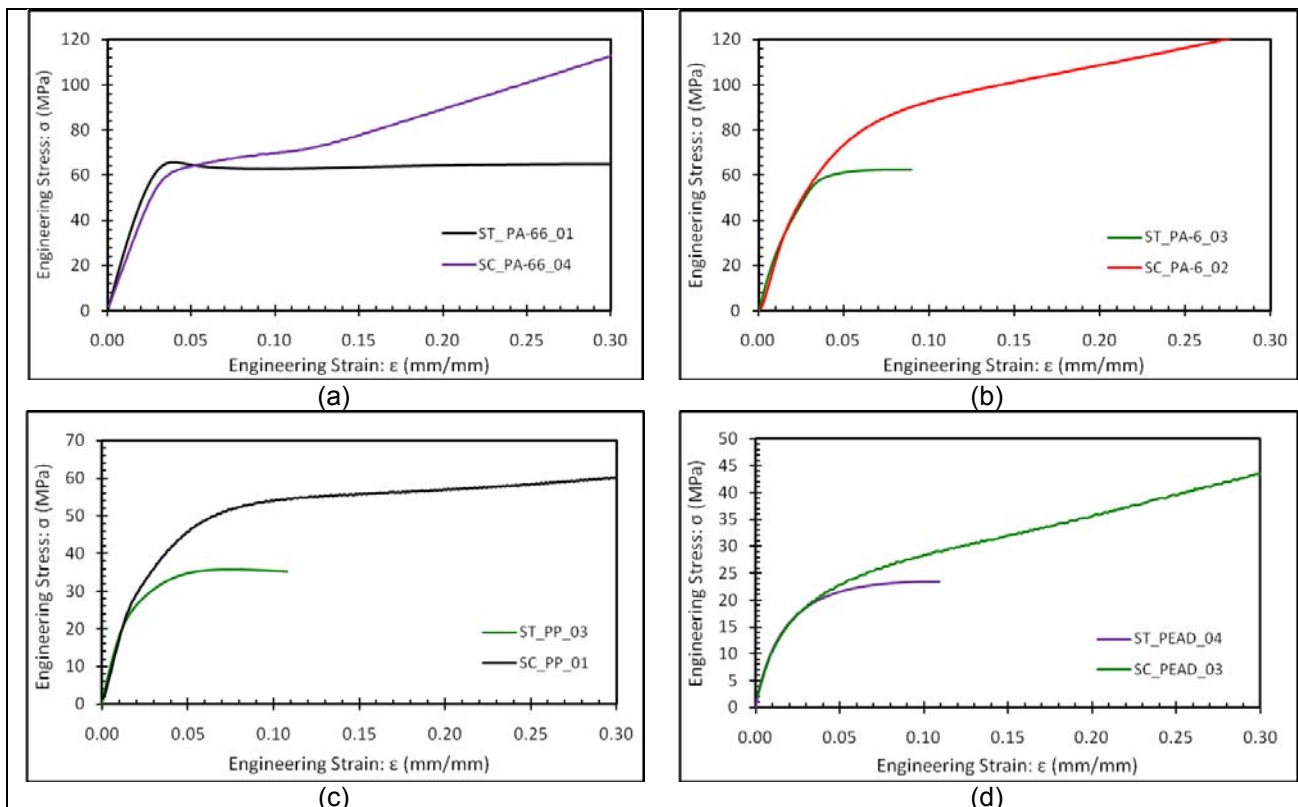


Figure 7. Comparison between stress-strain selected curves under tension and compression respectively for (a) PA-66, (b) PA-6, (c) PP and (d) HDPE. It can be noticed that yield strength unevenness is clear mainly for PA-6, PP and HDPE.

Table 2: Results for evaluated mechanical properties. Unevenness levels were calculated for both engineering (m_e) and true (m_t) stress-strain data. It can be noticed the reduction for true data

Engineering stress-strain data							
Material	E	$\sigma_{ys-0.2}$	$\sigma_{ys-0.5}$	$\sigma_{ys-1.0}$	$\sigma_{ys-2.0}$	$\sigma_{ys-m\acute{a}x}$	σ_{uts}
PA-66 Tension (MPa)	2766±270	46.7±8.9	57.6±5.4	63.3±2.0	64.9±1.0	64.6±1.1	61.3±8.3
PA-66 Compr. (MPa)	1984±90	53.8±1.3	59.1±0.3	63.5±2.9	64.9±0.4	69.5±3.3	---
m_e -PA-66	0.72±0.11	1.15±0.19	1.03±0.09	1.00±0.06	1.00±0.02	1.08±0.05	---
PA-6 Tension (MPa)	2871±209	34.3±5.8	43.7±5.1	52.9±3.2	60.4±0.9	63.3±0.8	63.3±0.8
PA-6 Compr. (MPa)	2340±61	45.0±0.9	53.6±0.9	63.7±0.9	75.3±0.8	107.5±0.7	---
m_e -PA-6	0.82±0.08	1.31±0.17	1.23±0.12	1.20±0.06	1.25±0.02	1.70±0.01	---
PP Tension (MPa)	1778±112	19.9±0.6	24.3±0.5	27.7±0.4	31.7±0.5	36.1±0.2	36.1±0.2
PP Compr. (MPa)	1682±91	27.6±1.1	31.7±1.0	36.9±0.8	44.1±0.6	55.9±0.1	---
m_e -PP	0.95±0.08	1.39±0.05	1.31±0.04	1.33±0.03	1.39±0.02	1.55±0.01	---
HDPE Tension (MPa)	1650±93	9.7±1.8	13.1±1.8	16.3±1.9	20.0±2.3	23.5±0.4	23.5±0.4
HDPE Compr. (MPa)	932±86	13.6±1.1	15.8±0.9	18.4±0.6	21.6±0.4	30.9±0.9	---
m_e -HDPE	0.56±0.11	1.40±0.20	1.21±0.15	1.13±0.12	1.08±0.12	1.31±0.03	---
True stress-strain data							
Material	E (MPa)	$\sigma_{ys-0.2}$	$\sigma_{ys-0.5}$	$\sigma_{ys-1.0}$	$\sigma_{ys-2.0}$	$\sigma_{ys-m\acute{a}x}$	σ_{uts}
PA-66 Tension (MPa)	---	48.3±7.1	59.8±4.1	65.9±1.7	67.0±1.0	67.2±1.1	---
PA-66 Compr. (MPa)	---	48.6±1.4	55.1±0.4	58.7±0.7	61.1±0.7	62.9±1.1	---
m_t -PA-66	---	1.01±0.15	0.92±0.07	0.89±0.03	0.91±0.02	0.94±0.02	---
PA-6 Tension (MPa)	---	36.0±6.5	46.0±5.6	55.7±3.1	63.4±0.9	68.7±0.9	---
PA-6 Compr. (MPa)	---	41.9±1.0	49.9±0.6	58.8±0.7	69.2±0.6	87.6±1.2	---
m_t -PA-6	---	1.16±0.18	1.08±0.12	1.06±0.06	1.09±0.02	1.27±0.02	---
PP Tension (MPa)	---	20.7±0.6	25.0±0.4	28.6±0.5	33.0±0.8	39.2±0.3	---
PP Compr. (MPa)	---	26.4±0.6	30.2±0.7	34.8±0.6	40.9±0.5	46.5±0.9	---
m_t -PP	---	1.27±0.04	1.21±0.03	1.22±0.02	1.24±0.03	1.19±0.02	---
HDPE Tension (MPa)	---	9.0±0.5	12.7±0.5	16.2±0.5	19.9±0.4	26.0±0.8	---
HDPE Compr. (MPa)	---	12.8±0.9	15.1±0.6	17.5±0.4	20.2±0.4	26.8±0.3	---
m_t -HDPE	---	1.42±0.10	1.19±0.06	1.08±0.04	1.02±0.03	1.03±0.03	---

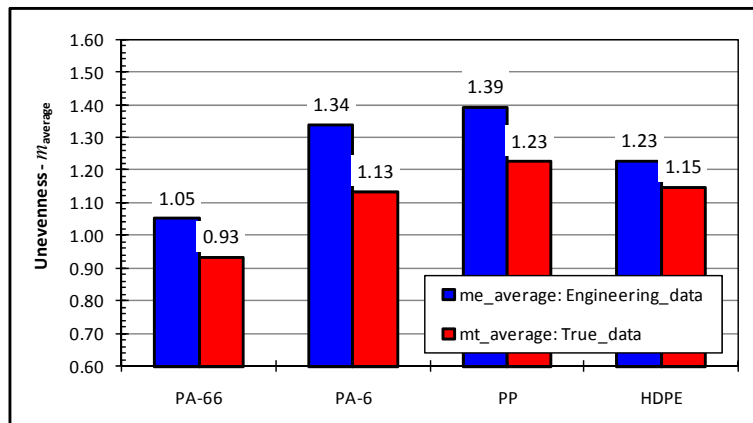


Figure 8. Average values of (m_e) and (m_t) considering all the definitions of σ_{ys} from Table 2. It can be realized that true values indicate less unevenness. They are considered here as more realistic.

5 EXPLORATORY DESIGN APPLICATION AND FINAL DISCUSSION

The experimental results presented in the previous section are of great interest for structural improvement of polymeric parts in mechanical engineering. To illustrate this potential, this section contains a brief exploratory application of uneven yield strength for design. In order to take advantage of this phenomenon, the component being designed must present regions loaded predominantly and permanently under compression. It means that loading cannot be cyclic (tensile-compressive) nor sometimes tensile. One example of a real component that presents regions under compression is the mechanical joining system called snap-fit. Snap-fits are polymeric union parts that can sometimes substitute screws and rivets and in its basic conception work as a cantilever beam, as shown by Figure 9(a). Figure 9(b) presents an illustrative usual cross section for simple snap-fits, which is rectangular and whose neutral axis is in the middle of its height (h). Considering that the beam is loaded by a force F (Figure 9(a)) and making use of Bernoulli's and elasticity theory,^(19,20) bending (σ) and shear (τ) stresses are maximum in the ABC plane (clamped region) and calculated neglecting stress intensity factors as

$$\sigma = \frac{F \cdot L \cdot h}{2 \cdot I}, \quad \tau = \frac{V \cdot Q}{I \cdot t} \quad (10)$$

where forces F and V and length L are fixed here ($F = V = 66$ N and $L = 25$ mm), I represents the moment of inertia, Q represents the static moment of area and t represents the width in the analyzed vertical position.⁽²⁰⁾ Based on Eqs. (10), equivalent stresses can be computed using Eqs. (4,7,8). Consequently, safety factor ($S.F.$) can be computed as $S.F. = \sigma_{ys-t} / \sigma_{equivalent}$.

Maximum bending stresses occur at the top and bottom fibers of the cross section, while maximum shear stress occurs at the neutral axis. Consequently, these three positions are analyzed here and characterize structural integrity. Due to practical application and technological interest, PP was selected for the exploratory investigation. Considering true stress-strain data and the 2.0 % offset method (highly representative of the average behavior of PP – see Table 2 and Figure 8), average elastic modulus for tension and compression is $E = 1730$ MPa, $\sigma_{ys-2.0-T} = 33.0$ MPa, $\sigma_{ys-2.0-C} = 33.0$ MPa and unevenness level is considered equal to $m = 1.24$.

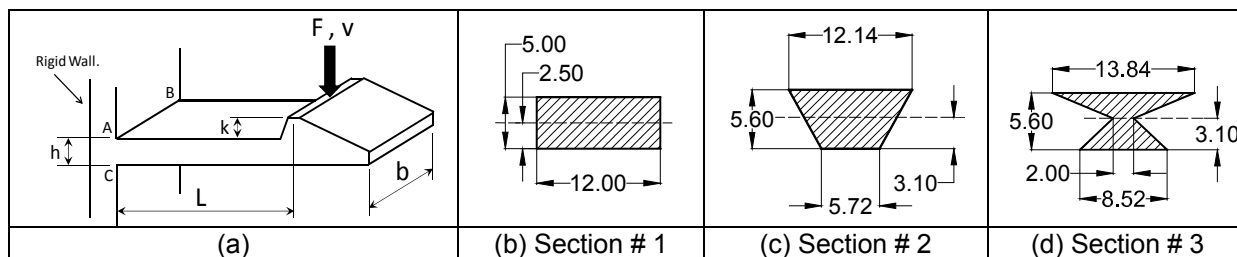


Figure 9. (a) Cantilever beam snap-fit, (b) usual rectangular cross section, (c) proposed trapezoidal and (d) proposed double trapezoidal cross sections. Neutral axes are indicated by the dashed lines.

To incorporate uneven properties in design and take advantage of larger compressive mechanical resistance, geometric changes were proposed for the original snap-fit cross section (Figure 9(b)) using optimization techniques. The main objective is to apply the modified criteria and try to establish unitary safety factors reducing mass and keeping stiffness. The parabolically modified criterion was adopted, Eq. 8, due to experimental better agreement according to the literature. Table 3 contains all the achieved results and will be discussed.

The original rectangular cross section is analyzed first (Section # 1, Figure 9(b)). From Beam theory it is well known that maximum normal stresses happen at the top and bottom fibers with same value but opposite signs, and that maximum shear stresses happen at the neutral axis. The second column of Table 3 shows that considering original von Mises criterion (vM), equivalent stresses at the top ($\sigma_{eq.-up}$) and bottom ($\sigma_{eq.-bottom}$) are considered the same and lead both to unitary safety factors ($S.F._{up} = S.F._{bottom} = 1.00$). When considering the parabolically modified criterion ($vM - P$), it can be realized in the third column that top fibers, which operate under tension, are not affected by the modified criterion (it can be seen in Figure 3(a) that for $\sigma_A/\sigma_{ys-t} = 1$ and $\sigma_B = 0$, all criteria converge). On the other hand, in the neutral axis (where loading is not uniaxial) and bottom fibers (where $\sigma_A/\sigma_{ys-t} = -1$) the different criteria diverge and safety factors are respectively $S.F._{axis} = 12.86$ and $S.F._{bottom} = 1.24$. Taking the bottom fiber as an example, this occurrence demonstrates that there is 24 % extra safety that was not accounted for by original Mises criterion and can be optimized, as is presented in the sequence. Moment of inertia (I) and cross section area for section #1 were used as a reference for the other proposals.

As the bottom fibers of the snap-fit operates under compression and present higher yield strength, one idea to illustrate the methodology is to turn the rectangular cross section into a trapezoidal one (Section # 2, Figure 9(c)). This geometrical change offsets neutral axis to a higher position and makes normal stresses at the bottom (compressive) larger than at the top (tensile). To determine geometric features for the cross section, a reduced gradient nonlinear optimization code (GRG2)⁽²¹⁾ was applied. The code enforced original stiffness (by keeping $I = 125 \text{ mm}^4$) and unitary safety factors at the top and bottom considering Mises parabolic model, providing the other geometric features to configure an optimum trapezoid. Results are presented in Table 3, columns 3 and 4. It can be realized that original Mises model predicts failure at the bottom ($S.F._{bottom} = 0.81$), while parabolic Mises model predicts $S.F._{bottom} = 1.00$. Consequently, keeping original stiffness and desired unitary safety factors, a mass reduction (area reduction) of 16.70 % was achieved.

However, the trapezoid was not a good option to improve the neutral axis region and safety factors there kept extremely high (larger than 10). For illustration purposes (neglecting cost or manufacturability), a third cross section (Section # 3, Figure 9(d))

was obtained using the same optimization techniques but allowing the algorithm to count on two trapezoids. A minimum neutral axis width was specified in 2.00 mm to avoid elastic instability and the other geometrical features emerged. The last two columns of Table 3 show that keeping the same original stiffness and safety factors, the mass reduction in this case achieved 39.8 %.

Table 3: Results the three evaluated cross sections presented by Figure 9. In each case, stresses and safety factors were computed using conventional (vM) and parabolically modified ($vM-P$) Von Mises

Parameter	Section # 1		Section # 2		Section # 3	
	vM	$vM-P$	vM	$vM-P$	vM	$vM-P$
$\sigma_{eq.-up}$ (MPa)	33.00	33.00	33.00	33.00	33.00	33.00
$\sigma_{eq.-axis}$ (MPa)	2.86	2.57	3.34	3.00	14.14	12.70
$\sigma_{eq.-bottom}$ (MPa)	33.00	26.63	40.90	33.00	40.90	33.00
$S.F._{up}$	1.00	1.00	1.00	1.00	1.00	1.00
$S.F._{axis}$	11.55	12.86	9.89	11.01	2.33	2.60
$S.F._{bottom}$	1.00	1.24	0.81	1.00	0.81	1.00
I (mm ⁴)	125 (<i>reference</i>)		125 (+ 0.00%)		125 (+ 0.00%)	
Section Area (mm ²)	60.00 (<i>reference</i>)		50.00 (- 16.70%)		36.10 (- 39.80%)	

6 CONCLUDING REMARKS

From this work it is possible to conclude that:

- Conically modified theory is more sensitive to high m values, which is expected due to the linear dependence on σ_h . However, for m values up to ~ 1.30 predictions from conical and parabolic models are analogous.
- All tested materials presented stiffness reduction under compression ($< E$).
- Considering deviation, only PA-66 presented even yield strength. PA-6, PP and HDPE presented unevenness levels between 23 % and 39 % considering engineering and 13 % and 23 % considering true properties.
- As strain levels are significant when evaluating yield strength, considering true stress-strain data is recommended for realism and safety.
- The incorporation of uneven polymer mechanical properties in design practices provided mass reductions up to 39.8 % keeping original stiffness and safety factors, which encourages future developments in the field.
- This calls the attention to the potential of critically investigating mechanical behavior of emerging materials in order to achieve structural improvement and cost reduction. Finite element and optimization codes, as well as experimental structural techniques, are essential for supporting future efforts.

Acknowledgment

This work is supported by Centro Universitário da FEI, São Paulo, Brazil.

REFERENCES

- 1 DOWLING, N. E. Mechanical Behavior of Materials - Engineering Methods for Deformation, Fracture and Fatigue, 2nd edition, Prentice Hall, New Jersey, USA, 1999.
- 2 ROESLER, J.; HARDERS, H.; BAEKER, M. Mechanical Behavior of Engineering Materials. Metals, Ceramics, Polymers and Composites. 1st edition, Springer, USA, 2007.
- 3 BOWER, D. I. An Introduction to Polymer Physics, Cambridge Press, USA, 2002.



- 4 WARD, I. M.; SWEENEY, J. An Introduction to the Mechanical Properties of Solid Polymers, New York, USA, 1972.
- 5 RAGHAVA, R.; CADDELL, R. M. The Macroscopic Yield Behavior of Polymers, University of Michigan, Ann Arbor, Michigan, USA, 1973.
- 6 CADDELL, R. M.; RAGHAVA, R. S.; ATKINS, A. G. Pressure Dependent Yield Criteria for Polymers, Materials Science and Engineering, V. 13, Issue 2, p. 113-120, 1974.
- 7 MASCARENHAS, W. N.; AHRENS, C. H.; OGLIARI, A. Design criteria and safety factors for plastic components design, Materials and Design, V. 25, p. 257-261, 2004.
- 8 JERABEK, M.; STEINBERGER, R.; MAJOR, Z. Characterization of the compression behaviour of engineering polymers, 22nd DANUBIA-ADRIA Symposium, Parma, Italy, 2005.
- 9 CES EDUPACK 2009 – Software for Materials Selection. Granta Design, website available at: <http://www.grantadesign.com/education/software.htm>, access in December, 2009.
- 10 HUBER, M. T. Theorie der Berührung fester elastischer Körper. Physik, 14/1, p.153-163, 1904.
- 11 HENCKY, H. Zur Theorie Plastischer Deformationen und der Hierdurch im Material Hervorgerufenen Nachspannungen, Angewandter Math. und Mech., 4, p. 323-334, 1924.
- 12 VON MISES, R. Mechanik der festen Körper im plastisch deformablen Zustand. Göttin. Nachr. Math. Phys., vol. 1, pp. 582-592, Germany, 1913.
- 13 LYON, R. E. Physical Basis for a Pressure-Dependent Yield Criterion for Polymers, U.S. Army Laboratory Command, Ballistic Research Laboratory, USA, 1992.
- 14 HU, L. W.; PAE, K. D. Inclusion of the Hydrostatic Stress Component in Formulation of the Yield Condition, Journal of Franklin Institute, V. 275, Issue 6, Pages 491-502, 1963.
- 15 EHRENSTEIN G. W.; ERHARD G. Designing with Plastic: a Report on the State of the Art, Carl Hanser Verlag, Munich, Germany, 1994.
- 16 MILLER, E. Introduction to Plastic and Composites: Mechanical Properties and Engineering Applications, Marcel Dekker Inc., New York, USA, 1996.
- 17 ASTM Standard D638 - 08. Standard Test Method for Tensile Properties of Plastics, USA, 2008.
- 18 ASTM Standard D695 - 08. Standard Test Method for Compressive Properties of Rigid Plastics, ASTM International, Pennsylvania, USA, 2008.
- 19 BEER, F. P., JOHNSTON, E. R., DEWOLF, J. T. Mechanics of Materials, 4th edition, 2005.
- 20 FÉODOSIEV, V. Résistance des Matériaux, Technique Soviétique, Moscow, 1977.
- 21 MS EXCEL, Solver: Generic Reduced Gradient Nonlinear Optimization Code (GRG2), 2007.